Available on the CERN CDS information server **CMS PAS SMP-12-001**

CMS Physics Analysis Summary

Contact: cms-pag-conveners-smp@cern.ch 2012/03/07

Measurement of the Electron Charge Asymmetry in Inclusive W Production in pp Collisions at $\sqrt{s} = 7\,\text{TeV}$

The CMS Collaboration

Abstract

A measurement of the electron charge asymmetry in inclusive $pp \to W + X$ production at $\sqrt{s} = 7\,\text{TeV}$ is presented based on data recorded by the CMS detector at the LHC and corresponding to an integrated luminosity of 840 pb^{-1}. The electron charge asymmetry is measured in eleven bins of absolute value of lepton pseudorapidity and it varies from 0.102 to 0.224. The total uncertainty on the measured asymmetry ranges between 0.006 and 0.014. This high precision measurement of the electron charge asymmetry provides new constraints into parton distribution functions.

In pp collisions, W bosons are produced primarily via the processes $u\bar{d} \to W^+$ and $d\bar{u} \to W^-$. The first quark is a valence quark from one of the protons, and the second one is a sea antiquark from the other proton. Due to the presence of two valence u quarks in the proton, there is an overall excess of W^+ over W^- bosons. The ratio of inclusive cross sections for W^+ and W^- bosons production at the Large Hadron Collider (LHC) was measured to be 1.42 ± 0.03 by the Compact Muon Solenoid (CMS) experiment [1] and is in agreement with predictions of the Standard Model (SM) based on various parton distribution functions (PDFs) [2, 3]. Measurement of this production asymmetry between W^+ and W^- bosons as a function of boson rapidity can provide better constraints on the u/d ratio and the sea antiquark densities in the ranges of the Björken parameter x [4] probed in pp collisions at $\sqrt{s} = 7\,\text{TeV}$. However, due to the presence of neutrinos in leptonic W decays the boson rapidity is not directly accessible. The experimentally accessible quantity is the lepton charge asymmetry, defined to be

$$\mathcal{A}(\eta) = \frac{\mathrm{d}\sigma/\mathrm{d}\eta(W^+ \to \ell^+\nu) - \mathrm{d}\sigma/\mathrm{d}\eta(W^- \to \ell^-\bar{\nu})}{\mathrm{d}\sigma/\mathrm{d}\eta(W^+ \to \ell^+\nu) + \mathrm{d}\sigma/\mathrm{d}\eta(W^- \to \ell^-\bar{\nu})},$$

where ℓ is the daughter charged lepton, η is the charged lepton pseudorapidity in the CMS lab frame ($\eta = -\ln[\tan(\frac{\theta}{2})]$ where θ is the polar angle), and $\mathrm{d}\sigma/\mathrm{d}\eta$ is the differential cross section for charged leptons from W boson decays. The lepton charge asymmetry can be used to test SM predictions with high precision.

The lepton charge asymmetry and the W charge asymmetry have been studied in $p\bar{p}$ collisions by both the CDF and D0 experiments at the Fermilab Tevatron Collider [5, 6]. ATLAS and CMS experiments have reported measurements of the lepton charge asymmetry at the LHC recently using the data collected during the 2010 LHC runs [7, 8]. CMS also reported an updated measurement of the muon charge asymmetry using a dataset corresponding to an integrated luminosity of 234 pb^{-1} including the full 2010 dataset and part of the 2011 dataset [9]. In this paper we present an update of the measurement of the electron charge asymmetry in inclusive $pp \to W(e\nu) + X$ production at $\sqrt{s} = 7$ TeV with a data sample corresponding to 840 pb^{-1} collected in Spring 2011. With respect to the analysis performed in 2010 [8] the threshold on the electron transverse momentum is increased from 25 to 35 GeV to match the updated trigger threshold for single electrons. The data sample is ~ 25 times larger than in 2010 and allows a reduction of many systematic uncertainties which were previously limited by the smaller amount of data.

A detailed description of the CMS experiment can be found elsewhere [10]. The central feature of the CMS apparatus is a superconducting solenoid, of 6 m internal diameter, 13 m in length, providing an axial field of 3.8 T. Within the field volume are the silicon pixel and strip tracker, the crystal electromagnetic calorimeter (ECAL) and the brass/scintillator hadron calorimeter (HCAL). Muons are measured in gas-ionization detectors embedded in the steel return yoke of the solenoid. The most relevant sub-detectors for this measurement are the ECAL and the tracking system. The electromagnetic calorimeter consists of nearly 76 000 lead tungstate crystals which provide coverage in pseudorapidity $|\eta| < 1.479$ in the barrel region and $1.479 < |\eta| < 3.0$ in two endcap regions. A preshower detector consisting of two planes of silicon sensors interleaved with a total of $3\,X_0$ of lead is located in front of the ECAL endcaps. The electron energy resolution is 3% or better for the range of electron energies relevant for this analysis. CMS uses a right-handed coordinate system, with the origin at the nominal interaction point, the x-axis pointing to the center of the LHC, the y-axis pointing up (perpendicular to the LHC plane), and the z-axis along the anticlockwise-beam direction. The polar angle, θ, is measured from the positive z-axis and the azimuthal angle, ϕ, is measured in the x-y plane.

The $W \to e\nu$ candidates are characterized by a high-p_T electron accompanied by missing transverse energy $\not{E}_T$, due to the escaping neutrino. Experimentally, $\not{E}_T$ is determined as the negative vector sum of the transverse momenta of all particles reconstructed using a particle flow algorithm [11] and, in this measurement, $\not{E}_T$ is used to separate signal from background on a statistical basis. The $W \to e\nu$ candidates used in this analysis were collected using a set of inclusive single-electron triggers which did not include $\not{E}_T$ requirements. Other physics processes, such as multijet and photon+jet production (QCD background), Drell–Yan ($Z/\gamma^* \to \ell^+\ell^-$) production, $W \to \tau\nu$ production (EWK background), and top quark pair ($t\bar{t}$) production can produce high-p_T electron candidates and mimic W candidates.

Monte Carlo (MC) simulation samples have been used to develop analysis techniques and estimate some of the background contributions. The W and Z bosonproduction and decays are simulated with the POWHEG [12] event generator interfaced with the CT10 [3] PDF model. The QCD multijet and $t\bar{t}$ backgrounds are generated with the PYTHIA [13] and MADGRAPH [14] event generators respectively. Both MADGRAPH and PYTHIA are interfaced with the CTEQ6L [15] PDF model. All generated events are passed through the CMS detector simulation using GEANT4 [16] and then processed using a reconstruction sequence identical to that used for collision data.

The selection criteria for electron reconstruction and identification are similar to those used in the W and Z cross section measurements [17]. A brief summary is given here for completeness. Electrons are identified as clusters of energy deposited in the ECAL fiducial volume matched to tracks from the inner silicon tracker. The tracks are reconstructed using a Gaussian-Sum-Filter (GSF) algorithm [18] that takes into account possible energy loss due to bremsstrahlung in the tracker layers. Particles misidentified as electrons are suppressed by requiring that the shower shape of the ECAL cluster be consistent with an electron candidate, and that the η and ϕ coordinates of the track trajectory extrapolated to the ECAL match the η and ϕ coordinates of the ECAL cluster. Furthermore, electrons from W decay are isolated from other activity in the event. We therefore require that little transverse energy be observed in the ECAL, HCAL, and silicon tracking system within a cone $\Delta R < 0.3$ around the electron direction, where $\Delta R = \sqrt{(\Delta\phi)^2 + (\Delta\eta)^2}$ and where calorimeter energy deposits and the track associated with the electron candidate are excluded. Due to the substantial amount of material in front of the ECAL detector, a large fraction of electrons radiate photons. The resulting photons may convert close to the original electron trajectory, leading to a sizable charge misidentification rate (w). Three different methods are used to determine the electron charge. First, the electron charge is determined by the signed curvature of the associated GSF track. Second, the charge is determined from the associated trajectory reconstructed in the silicon tracker using a Kalman Filter algorithm [19]. Third, the electron charge is determined based on the azimuthal angle between the vector joining the nominal interaction point and the ECAL cluster position and the vector joining the nominal interaction point and innermost hit of the GSF track. It is required that all three charge determinations from these methods agree. This procedure significantly reduces the charge misidentification rate to 0.01% in the ECAL barrel and to 0.3% in the ECAL endcaps. The $W \to e\nu$ candidates are selected by requiring electrons to have $p_T > 35\,\text{GeV}/c$, $|\eta| < 2.4$ and to be associated with one of the electron trigger candidates used to select the electron dataset. The Drell–Yan and $t\bar{t}$ backgrounds are suppressed by rejecting events that contain a second isolated electron or muon with $p_T > 15\,\text{GeV}/c$ and $|\eta| < 2.4$. According to MC simulations, the data sample of selected electrons consists of about 16 % QCD background events, about 7.4% EWK background events, and about 0.4% $t\bar{t}$ background events. The events passing the above selection criteria are divided into bins of electron pseudorapidity. The width of the bin is 0.2 and the pseudorapidity region between 1.4 and 1.6 is excluded because it corresponds

to the transition region between the ECAL barrel and endcaps.

A binned extended maximum likelihood fit is performed to the $\not\!\!E_T$ distribution to estimate the $W \to e\nu$ signal yield for electrons (N^-) and positrons (N^+) in each pseudorapidity bin. The signal $\not\!\!E_T$ shape is derived from MC simulations with an event-by-event correction to account for energy scale and resolution differences between data and MC inferred from the hadronic recoil energy distributions in $Z/\gamma^* \to e^+e^-$ events selected from data [20]. The shape of the QCD background is determined, for each charge, from a signal-free control sample obtained by inverting a subset of the electron identification criteria. The $\not\!\!E_T$ shapes for other backgrounds such as the Drell–Yan process, $t\bar{t}$, and $W \to \tau\nu$ are taken from MC simulations with a fixed normalization relative to the $W \to e\nu$ yields. The normalization factors are calculated from the predicted values of the cross sections at NLO. The yield of the QCD background and the yield of the $W \to e\nu$ signal (N) are free parameters in the fit. The results of the fits to the data are shown for the first and for the tenth pseudorapidity bin in Fig. 1. The uncertainty in each bin represents the systematic and statistical error associated to the N extraction procedure. The charge asymmetry is obtained from $(N^+ - N^-)/(N^+ + N^-)$.

There are two sources of systematic uncertainty relating to the signal $\not\!\!E_T$ shape, the PDF used to generate the events and the uncertainty on the recoil corrections applied to the events. The PDF uncertainty is evaluated using the CTEQ6.6 uncertainty PDFs which contain the central PDF and the upper and lower uncertainty PDFs for 22 parameters. The PDFs uncertainties are combined using the prescription given by the PDF4LHC Working Group [21]. Uncertanties on the recoil corrections are propagated to generate different templates and studying their effect on the measured asymmetry. The systematic uncertainty due to the QCD background shape is studied by using different QCD background control regions to derive the QCD background $\not\!\!E_T$ shape. The effect on the asymmetry is estimated to be $1 - 2 \times 10^{-3}$. The systematic uncertainty due to the modeling of Drell-Yan, $t\bar{t}$, and $W \to \tau\nu$ are evaluated by varying the relative normalization of the EWK backgrounds to the $W \to e\nu$ yield by the uncertainty on the Drell-Yan and $t\bar{t}$ cross sections, and the effect on the observed asymmetry is negligible. The values of (N) from the fitting procedure are insensitive to the presence of pile-up interactions thanks to the use of data-driven $\not\!\!E_T$ templates.

In order to compare our results directly to theoretical predictions, the observed charge asymmetry is corrected for three detector effects: 1) electron energy scale and resolution, 2) relative detection efficiency of positrons and electrons, 3) electron charge misidentification.

The electron energy scale and resolution can bias the asymmetry, due to the effect for leptons with a transverse momentum close to the threshold at 35 GeV applied in this analysis. The electron energy scale and resolution are determined directly from the $Z/\gamma^* \to e^+e^-$ data and are used to smear MC electron energy at the generator level. The correction to the measured charge asymmetry is estimated in each pseudorapidity bin by comparing the charge asymmetry as determined in the MC with the resulting asymmetry after smearing. The corrections for the electron energy scale and resolution are found to fall between -4.4 $\times 10^{-3}$ and 0.2 $\times 10^{-3}$. The uncertainties on the energy scale and resolutions are taken as sources for systematic uncertainties. The charge asymmetry is also corrected for the final state radiation and the uncertainty on the correction is taken as additional systematic uncertainty which is summed in quadrature with the lepton energy scale systematic uncertainty.

Any efficiency difference between electrons and positrons would bias the measured charge asymmetry. The total electron efficiency (including electron reconstruction, identification, and trigger efficiencies) in each pseudorapidity bin is measured using the $Z/\gamma^* \to e^+e^-$ data for e^+ and e^-, respectively. The efficiency ratio is calculated and found to be between 0.96 and 1.03

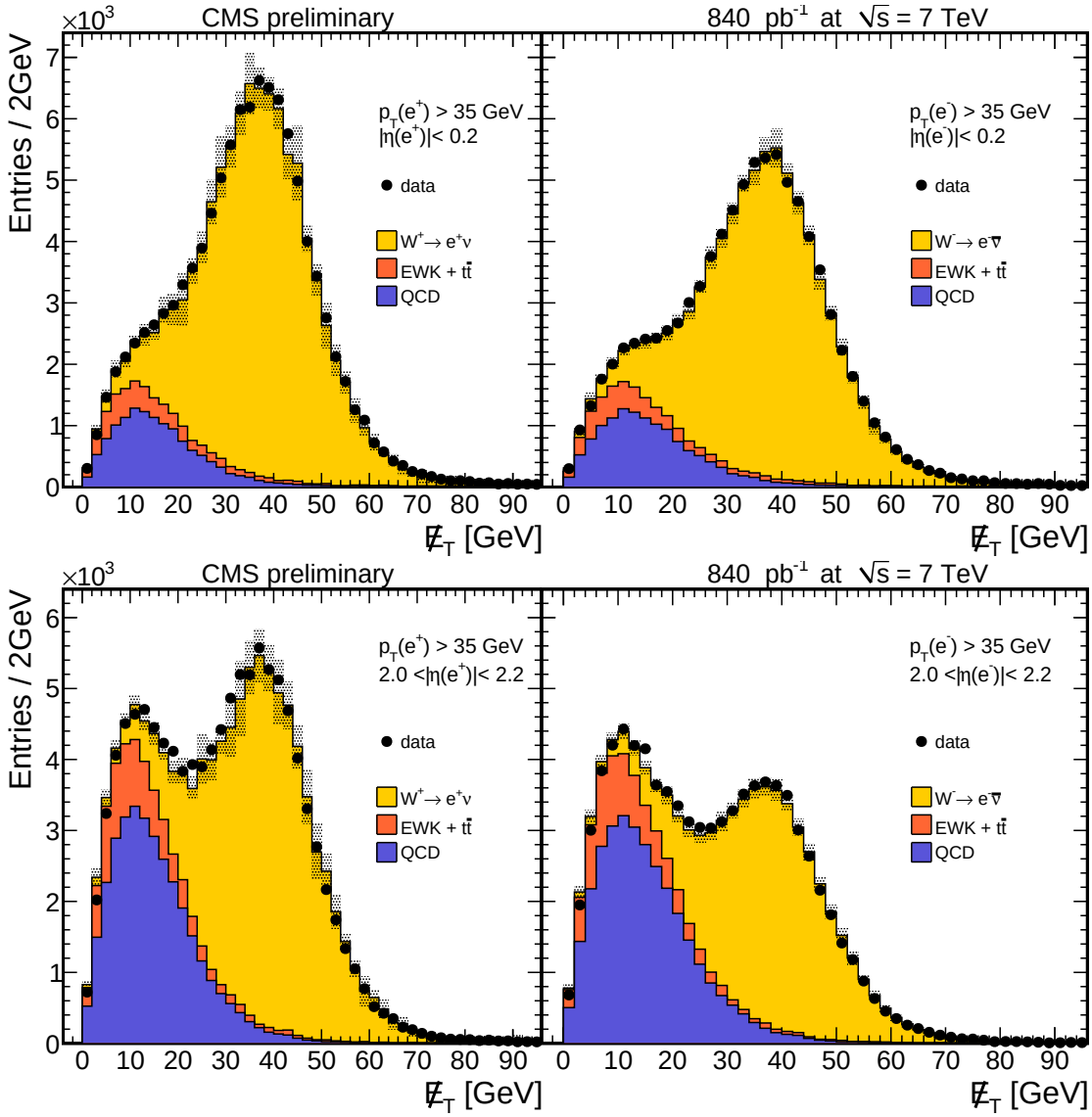

Figure 1: Signal fit to data $\not\!\!E_T$ distributions for electrons. Results for the first pseudorapidity bin ($|\eta| < 0.2$) and for the 10th pseudorapidity bin ($2.0 < |\eta| < 2.2$) are shown. The hatched area represents the statistical and systematic uncertainties associated to the fitting procedure.

and the statistical errors on the efficiency ratios are treated as systematic uncertainties. This is the dominant systematic uncertainty in all the pseudorapidity bins.

The true charge asymmetry, $\mathcal{A}$, is diluted due to charge misidentification resulting in an observed asymmetry, $\mathcal{A}^{\rm obs} = \mathcal{A}(1-2w)$. The electron charge misidentification rate w is measured in data using $Z/\gamma^* \to e^+e^-$ evens. The observed electron charge asymmetry is corrected for the charge misidentification rate as a function of $|\eta|$. The statistical error on the electron charge misidentification rate is taken as the systematic uncertainty.

Table 1 summarizes systematic uncertainties in all the electron pseudorapidity bins. The full covariance systematic errors matrix is given in Table 2. The measured charge asymmetry results are summarized in Table 3 with both statistical and systematic uncertainties shown. The statistical uncertanties in the various pseudorapidity bins are uncorrelated.

Table 1: Summary of the systematic uncertainties. All values are in units $\times 10^{-3}$.

	Signal Yield	Energy Scale and Res.	Charge MisId.	Efficiency Ratio
$0.0 < \|\eta\| < 0.2$	1.8	0.6	0.0	4.5
$0.2 < \|\eta\| < 0.4$	2.5	0.6	0.0	4.4
$0.4 < \|\eta\| < 0.6$	2.7	0.3	0.0	4.4
$0.6 < \|\eta\| < 0.8$	2.5	0.3	0.0	4.4
$0.8 < \|\eta\| < 1.0$	1.9	0.6	0.1	4.4
$1.0 < \|\eta\| < 1.2$	2.4	1.0	0.1	4.9
$1.2 < \|\eta\| < 1.4$	2.6	0.8	0.1	5.4
$1.6 < \|\eta\| < 1.8$	3.1	0.8	0.1	9.2
$1.8 < \|\eta\| < 2.0$	2.0	1.6	0.2	8.7
$2.0 < \|\eta\| < 2.2$	2.0	2.6	0.3	10.0
$2.2 < \|\eta\| < 2.4$	2.9	2.4	0.3	12.5

Table 2: Covariance matrix for all the systematic errors. All the values are given in units $\times 10^{-6}$

	[0.0, 0.2]	[0.2, 0.4]	[0.4, 0.6]	[0.6, 0.8]	[0.8, 1.0]	[1.0, 1.2]	[1.2, 1.4]	[1.6, 1.8]	[1.8, 2.0]	[2.0, 2.2]	[2.2, 2.4]
[0.0, 0.2]	23.7	2.6	2.2	2.5	2.7	2.9	2.9	2.9	2.8	3.1	4.2
[0.2, 0.4]	2.6	26.2	2.6	2.9	3.1	3.3	3.4	3.2	3.0	3.9	4.7
[0.4, 0.6]	2.2	2.6	26.6	2.6	2.8	2.9	3.2	2.9	2.5	3.3	4.1
[0.6, 0.8]	2.5	2.9	2.6	25.6	3.3	3.4	3.7	3.3	2.8	3.7	4.7
[0.8, 1.0]	2.7	3.1	2.8	3.3	23.3	3.9	4.2	3.7	3.4	4.6	5.6
[1.0, 1.2]	2.9	3.3	2.9	3.4	3.9	30.8	4.5	4.1	4.0	5.7	6.8
[1.2, 1.4]	2.9	3.4	3.2	3.7	4.2	4.5	36.5	4.3	3.7	5.8	6.7
[1.6, 1.8]	2.9	3.2	2.9	3.3	3.7	4.1	4.3	94.9	3.8	5.1	6.2
[1.8, 2.0]	2.8	3.0	2.5	2.8	3.4	4.0	3.7	3.8	82.4	6.2	7.0
[2.0, 2.2]	3.1	3.9	3.3	3.7	4.6	5.7	5.8	5.1	6.2	110.7	10.3
[2.2, 2.4]	4.2	4.7	4.1	4.7	5.6	6.8	6.7	6.2	7.0	10.3	171.0

The experimental results are compared in Table 3 and in Fig. 2 to theoretical predictions obtained using MCFM [22] generator interfaced with CT10 [3], MSTW2008NLO [2], NNPDF [23], HERAPDF [24] PDF models. The theory PDF errors are estimated using the PDF reweighting technique [25]. The experimental data are in agreement with the predictions from CTEQ, NNPDF and HERAPDF, while the predictions from MSTW are systematically lower than the observed asymmetry. A similar inconsistency between data and MSTW predictions was observed in the muon charge asymmetry measurement presented recently by the CMS collaboration [9].

In summary, we have measured the electron charge asymmetry in the $W \to e\nu$ channel using a data sample corresponding to an integrated luminosity of 840 pb^{-1} collected with the CMS detector at the LHC. The uncertainty on the measured asymmetry ranges from 0.006 in the central region to 0.014 in the ECAL endcap. This high precision measurement of the W lepton charge asymmetry at the LHC provides new inputs to the PDF global fits.

Table 3: Summary of the measured charge asymmetry results ($\mathcal{A}$) . The first uncertainty is statistical and the second is systematic. The theoretical predictions are obtained using MCFM interfaced with 4 different PDF models. The PDF uncertainties are estimated using the PDF reweighting technique. All values are in units $\times 10^{-3}$.

	Measured	Theory Prediction			
	Asymmetry ($\mathcal{A}$)	CT10	HERAPDF	MSTW	NNPDF
$0.0 < \|\eta\| < 0.2$	$102 \pm 3 \pm 5$	109^{+5}_{-5}	106^{+4}_{-8}	83^{+3}_{-5}	107 ± 5
$0.2 < \|\eta\| < 0.4$	$111 \pm 3 \pm 5$	114^{+5}_{-5}	110^{+4}_{-8}	85^{+3}_{-5}	110 ± 5
$0.4 < \|\eta\| < 0.6$	$116 \pm 3 \pm 5$	119^{+5}_{-5}	115^{+4}_{-8}	92^{+3}_{-5}	116 ± 5
$0.6 < \|\eta\| < 0.8$	$123 \pm 3 \pm 5$	126^{+5}_{-5}	122^{+4}_{-8}	98^{+3}_{-5}	123 ± 5
$0.8 < \|\eta\| < 1.0$	$133 \pm 3 \pm 5$	138^{+5}_{-6}	132^{+4}_{-8}	108^{+4}_{-5}	134 ± 5
$1.0 < \|\eta\| < 1.2$	$136 \pm 3 \pm 6$	146^{+6}_{-6}	140^{+5}_{-8}	120^{+4}_{-5}	145 ± 5
$1.2 < \|\eta\| < 1.4$	$156 \pm 3 \pm 6$	164^{+6}_{-7}	153^{+5}_{-7}	136^{+5}_{-5}	158 ± 5
$1.6 < \|\eta\| < 1.8$	$166 \pm 3 \pm 10$	195^{+8}_{-9}	181^{+5}_{-5}	168^{+5}_{-5}	190 ± 4
$1.8 < \|\eta\| < 2.0$	$197 \pm 3 \pm 9$	207^{+8}_{-10}	196^{+4}_{-3}	184^{+6}_{-5}	206 ± 4
$2.0 < \|\eta\| < 2.2$	$224 \pm 3 \pm 11$	224^{+8}_{-11}	211^{+5}_{-3}	198^{+6}_{-5}	219 ± 4
$2.2 < \|\eta\| < 2.4$	$210 \pm 4 \pm 13$	241^{+8}_{-12}	225^{+9}_{-4}	214^{+6}_{-5}	231 ± 5

1 Acknowledgements

We wish to congratulate our colleagues in the CERN accelerator departments for the excellent performance of the LHC machine. We thank the technical and administrative staff at CERN and other CMS institutes, and acknowledge support from: FMSR (Austria); FNRS and FWO (Belgium); CNPq, CAPES, FAPERJ, and FAPESP (Brazil); MES (Bulgaria); CERN; CAS, MoST, and NSFC (China); COLCIENCIAS (Colombia); MSES (Croatia); RPF (Cyprus); Academy of Sciences and NICPB (Estonia); Academy of Finland, ME, and HIP (Finland); CEA and CNRS/IN2P3 (France); BMBF, DFG, and HGF (Germany); GSRT (Greece); OTKA and NKTH (Hungary); DAE and DST (India); IPM (Iran); SFI (Ireland); INFN (Italy); NRF and WCU (Korea); LAS (Lithuania); CINVESTAV, CONACYT, SEP, and UASLP-FAI (Mexico); PAEC (Pakistan); SCSR (Poland); FCT (Portugal); JINR (Armenia, Belarus, Georgia, Ukraine, Uzbekistan); MST and MAE (Russia); MSTD (Serbia); MICINN and CPAN (Spain); Swiss Funding Agencies (Switzerland); NSC (Taipei); TUBITAK and TAEK (Turkey); STFC (United Kingdom); DOE and NSF (USA).

References

[1] CMS Collaboration Collaboration, "Measurement of the Inclusive W and Z Production Cross Sections in pp Collisions at sqrt(s) = 7 TeV", *JHEP* **1110** (2011) 132. doi:10.1007/JHEP10(2011)132.

[2] A. D. Martin, W. J. Stirling, R. S. Thorne et al., "Parton distributions for the LHC", *Eur. Phys. J.* **C63** (2009) 189–285, arXiv:0901.0002. doi:10.1140/epjc/s10052-009-1072-5.

[3] H.-L. Lai et al., "New parton distributions for collider physics", *Phys. Rev.* **D82** (2010) 074024, arXiv:1007.2241. doi:10.1103/PhysRevD.82.074024.

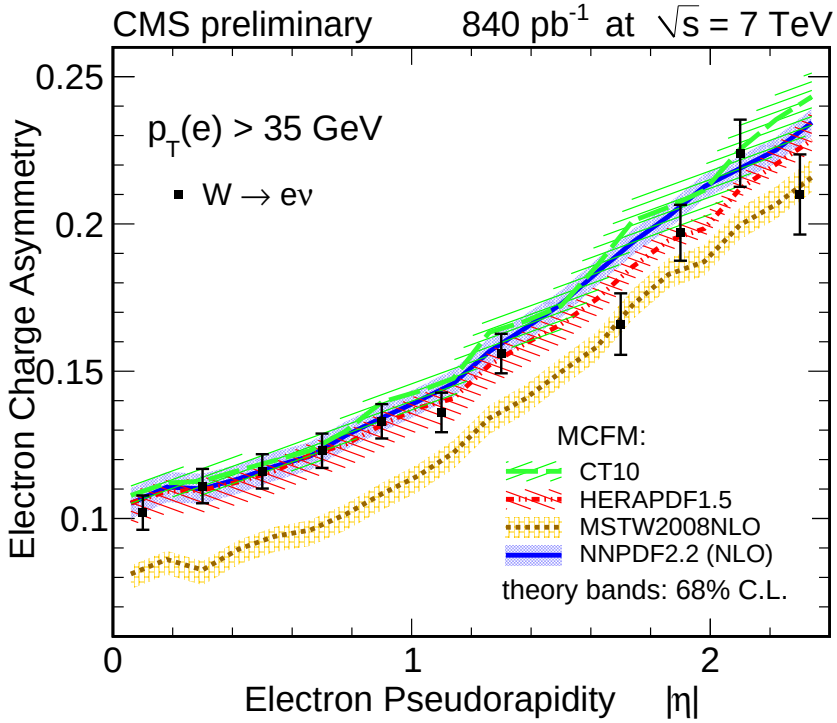

Figure 2: Comparison of the measured lepton charge asymmetry to different PDF models for electron $p_{\mathrm{T}}^{\ell} > 35\,\mathrm{GeV}/c$. The error bars include both statistical and systematic uncertainties. The data points are placed in the center of the eta bins. The PDF uncertainty band is estimated using the PDF reweighting technique and corresponds to 68% of confidence level.

[4] J. D. Björken and E. A. Paschos, "Inelastic Electron Proton and gamma Proton Scattering, and the Structure of the Nucleon", *Phys. Rev.* **185** (1969) 1975–1982. doi:10.1103/PhysRev.185.1975.

[5] CDF Collaboration, "Direct Measurement of the W Production Charge Asymmetry in $p\bar{p}$ Collisions at $\sqrt{s} = 1.96$ TeV", *Phys. Rev. Lett.* **102** (2009) 181801, arXiv:0901.2169. doi:10.1103/PhysRevLett.102.181801.

[6] D0 Collaboration, "Measurement of the electron charge asymmetry in $p\bar{p} \to W + X \to e\nu + X$ events at $\sqrt{s}$ = 1.96-TeV", *Phys. Rev. Lett.* **101** (2008) 211801, arXiv:0807.3367. doi:10.1103/PhysRevLett.101.211801.

[7] ATLAS Collaboration, "Measurement of the Muon Charge Asymmetry from W Bosons Produced in pp Collisions at sqrt(s) = 7 TeV with the ATLAS detector", *Phys. Lett.* **B701** (2011) 31–49, arXiv:1103.2929. doi:10.1016/j.physletb.2011.05.024.

[8] CMS Collaboration, "Measurement of the lepton charge asymmetry in inclusive W production in pp collisions at sqrt(s) = 7 TeV", *JHEP* **04** (2011) 050, arXiv:1103.3470. doi:10.1007/JHEP04(2011)050.

[9] CMS Collaboration, "Measurement of the Muon Charge Asymmetry in Inclusive W Production in pp Collisions at $\sqrt{s}$=7 TeV", *CMS PAS* **EWK-11-005** (2010).

[10] CMS Collaboration, "The CMS experiment at the CERN LHC", *JINST* **0803:S08004** (2008).

[11] CMS Collaboration, "Particle-flow commissioning with muons and electrons from J/Psi, and W events at 7 TeV", *CMS PAS* **PFT-10-003** (2010).

[12] S. Frixione, P. Nason, and C. Oleari, "Matching NLO QCD computations with Parton Shower simulations: the POWHEG method", *JHEP* **11** (2007) 070, arXiv:0709.2092. doi:10.1088/1126-6708/2007/11/070.

[13] T. Sjöstrand, S. Mrenna, and P. Z. Skands, "PYTHIA 6.4 Physics and Manual", *JHEP* **05** (2006) 026, arXiv:hep-ph/0603175. doi:10.1088/1126-6708/2006/05/026.

[14] J. Alwall, M. Herquet, F. Maltoni et al., "MadGraph 5 : Going Beyond", *JHEP* **1106** (2011) 128, arXiv:1106.0522. doi:10.1007/JHEP06(2011)128.

[15] J. Pumplin et al., "New generation of parton distributions with uncertainties from global QCD analysis", *JHEP* **07** (2002) 012, arXiv:hep-ph/0201195.

[16] GEANT4 Collaboration, "GEANT4: A simulation toolkit", *Nucl. Instrum. Meth.* **A506** (2003) 250–303. doi:10.1016/S0168-9002(03)01368-8.

[17] CMS Collaboration, "Measurements of Inclusive W and Z Cross Sections in pp Collisions at $\sqrt{s}$ = 7 TeV", *JHEP* **2** (2011) 2–40, arXiv:hep-ph/10122466. doi:10.1007/JHEP01(2011)080.

[18] W. Adam et al., "Reconstruction of Electrons with the Gaussian-Sum Filter in the CMS Tracker at the LHC", *CMS Note* **2005/001** (2005).

[19] CMS Collaboration, "CMS Tracking Performance Results from early LHC Operation", *Eur. Phys. J.* **C70** (2010) 1165–1192, arXiv:1007.1988. doi:10.1140/epjc/s10052-010-1491-3.

[20] CMS Collaboration, "CMS MET Performance in Events Containing Electroweak Bosons from pp Collisions at $\sqrt{s}$=7 TeV", *CMS PAS* **JME-10-005** (2010).

[21] M. Botje, J. Butterworth, A. Cooper-Sarkar et al., "The PDF4LHC Working Group Interim Recommendations", arXiv:1101.0538.

[22] J. M. Campbell and R. K. Ellis, "Radiative corrections to Z b anti-b production", *Phys. Rev.* **D62** (2000) 114012, arXiv:hep-ph/0006304. doi:10.1103/PhysRevD.62.114012.

[23] R. D. Ball, V. Bertone, F. Cerutti et al., "Reweighting and Unweighting of Parton Distributions and the LHC W lepton asymmetry data", *Nucl.Phys.* **B855** (2012) 608–638, arXiv:1108.1758. doi:10.1016/j.nuclphysb.2011.10.018.

[24] H1 and ZEUS Collaboration Collaboration, "Combined Measurement and QCD Analysis of the Inclusive e+- p Scattering Cross Sections at HERA", *JHEP* **1001** (2010) 109, arXiv:0911.0884. doi:10.1007/JHEP01(2010)109.

[25] D. Bourilkov, R. C. Group, and M. R. Whalley, "LHAPDF: PDF use from the Tevatron to the LHC", arXiv:hep-ph/0605240.